Five-fold symmetry in fractal atom hydrogen probed with accurate 1S-nS terms

G. Van Hooydonk,
Ghent University, Faculty of Sciences, Ghent, Belgium

Abstract. We probe Penrose's five-fold symmetry and fractal behavior for atom H. With radius r_H derived from H mass m_H, H symmetry is governed by Euclid's golden ratio [sqrt(5)-1]/2, as proved with accurate H terms. Our prediction for H 1S-3S, to be measured soon, is 2 922 743 278 654 kHz.

I. Introduction

Euclid-Phidias numbers appear in fundamental and applied sciences, in arts… [1-3], and for chaotic or fractal behavior (Mandelbrot [4], Gutzwiller [5]) and Penrose's 5-fold symmetry [6]. With (1-x)/x =x/1 for complementary parts +x, 1-x of composite units, Euclidean harmony is $x_\pm=\varphi_\pm=-½(1\pm\sqrt{5})$. The simplest, smallest but most abundant neutral unit in the Universe [7], composite H has electron (mass m_e) and proton (mass m_P) as complementary parts: $m_H=m_e+m_P=m_e+(m_H-m_e)$ or 1=x+ (1-x), if $x=m_e/m_H$. If φ applied to H, it must show in its spectrum. By its compact nature, Bohr theory fails on φ-symmetry, also invisible in bound state QED [8]. We probe φ for H using mass m_H and radius r_H related by $m_H= (4\pi/3)\,\gamma r_H^3$. Scaling H levels by virial $½e^2/r_H$ gives away φ and fractal behavior. This is in line with Rydberg's original formula [9] and confirmed with accurate H 1S-nS terms [10]. We predict a value of 2922743278654 kHz for H 1S-3S, to be measured in the near future [11].

II. Rydberg equation and fractal behavior of atom H

II.1 Chaotic/fractal interpretation of the Rydberg formula for composite H

With constant a in Å and line number n, the original Rydberg formula [9] for H terms

$$T_n=an^2/(n^2-1)\text{ Å or } T_n/(an) =n/(n^2-1) =1/(n-1/n) \quad (1)$$

suggests that H may well exhibit fractal or chaotic behavior [4,5]. Bohr energy differences

$$\Delta E_n=1/T_n= (n^2-1)10^8/(an^2) =R_H (1-1/n^2)=R_H-R_H/n_2=E_n-E_1 \text{ cm}^{-1} \quad (2)$$

with Rydberg $R_H=10^8/a$ cm^{-1}, give fractal behavior (1) in linear form

$$n\Delta E_n/R_H=(n-1)(n+1)/n=n-1/n \quad (3)$$

With E_n [12] instead of ΔE_n, plots of nE_n versus n and 1/n give power laws

$$E_n(n)\equiv E_n(1/n)=109679{,}223605211n^{-1{,}000004252339}\equiv 109679{,}223605211(1/n)^{1{,}000004252339} \quad (4)$$

Linear n and inverse 1/n views suggest fractal H (3) within 0,007 cm^{-1}, while Bohr $1/n^2$ theory has errors of 0,0126 cm^{-1} (a power fit in $1/n^2$ has its exponent shifted by 1). The greatest difference with Bohr theory and QED is asymptote 109679,2236 cm^{-1} in (4), larger than $-E_1$=109678,773704 cm^{-1} in [12]. Since 1/n secures convergence, a 4th order fit in 1/n

$$nE_n=0{,}006889343262/n^4-4{,}375765800476/n^3+5{,}5580713748932/n^2+109677{,}585385323000/n \quad (5)$$

is accurate within 10^{-8} cm^{-1} or 0,45 kHz (less precise data [13] behave similarly). By its precision, (5) for fractal H must be important for metrology [10, 14-15], as we discuss further below.

II.2 Generalizing Bohr H theory and reduced mass: opening for φ

To not to interrupt the argument on φ, we compare H theories in Appendix A. With (A1)-(A2), Bohr's integer quantum number n and Rydberg R_H give rotational level energies

$$E_n=-R_H/n^2=-½(\hbar^2/\mu e^2)/n^2=-½\mu\alpha^2c^2/n^2=-½(e^2/r_0)/n^2 \quad (6)$$

Here, r_0 is Bohr radius $r_B=\hbar^2/(m_e e^2)$, corrected for reduced electron mass, according to

$$\mu=m_e m_P/(m_e+m_P)=m_e m_P/m_H=m_e/(1+m_e/m_P)\equiv m_e(1-m_e/m_H) \quad (7)$$

Generalizing (6) with a critical n_c for another H radius r_H by means of

$$r_H=n_c^2 r_0 \quad (8)$$

$$E_n=-(R_H/n_c^2)(\surd n_c/n)^2=-½[e^2/(n_c^2r_0)](\surd n_c/n)^2=-½(e^2/r_H)(\surd n_c/n)^2 \quad (9)$$

allows an infinite number of solutions, trivial or not.

(i) Any n_c (except 0) will lead to the same accuracy as (6). A relation between n_c and φ like

$$n_c=A\varphi^m \quad (10)$$

for (9) may probe Euclidean symmetry, but only if an alternative r_H existed (see Section II.3).

(ii) Detecting internal φ-effects in H depends on specific φ-relations [2-5] like

$$\varphi^{m+2}+\varphi^{m+1}=\varphi^m;\ 1=1/\varphi-\varphi;\ \varphi^2+\varphi-1=0 \text{ and } \varphi(\varphi+1)=1 \quad (11)$$

Internal φ-symmetries (11) are available from (7) in dimensionless form. With m_H, this gives product

$$\varrho_H=\mu/m_H=(m_e/m_H)(1-m_e/m_H)=x(1-x) \quad (12)$$

for parts ($d\varrho/dx=1-2x=0$ gives $\varrho_{max}=¼$ when $x=½$ or parts are equal; $\varrho=x(1-x)$ or $x^2-x+\varrho=0$ gives $x_\pm=½[1\pm\surd(1-4\varrho)]$); a center between parts leads to $-x$, $(1-x)$, $x^2-x+\varrho=0$ and $x_\pm=½[1\pm\surd(1+4\varrho)]$).

With only part ratios, all symmetries in (ii) are Euclidean (see Introduction).

By virtue of (10)-(12), reduced mass for H (12) implies Euclidean harmony between parts, obeying

$$\varrho_H=x(1-x)\sim A\varphi^m(1-A\varphi^m) \quad (13)$$

If valid, these are only small corrections to E_n, since μ/m_e (7) is 1837 times larger than μ/m_H (12).

The fate of H symmetries (9)-(13) depends solely on the existence of a valid alternative radius r_H.

II.3 Alternative classical H radius r_H

Apart from [16], a first principles alternative quantum radius for H, other than Bohr length r_B, does not exist. Only a classical 19th century macroscopic view on spherical H can give r_H using

$$m_H=(4\pi/3)\gamma r_H^3 \text{ and } r_H=[(3/4\pi\gamma)m_H]^{1/3} \quad (14)$$

where $4\pi/3$ is the form factor for a sphere and γ in g/cm^3 is H density.

With $m_H=m_e+m_P=9,10938215.10^{-28}+1,672621637.10^{-24}$ g [10] and $\gamma=1$ g/cm^3 for H, the result is

$$r_H=7,36515437.10^{-9} \text{ cm} = 0,736515437 \text{ Å} \quad (15)$$

This is the only real, theoretically possible alternative to Bohr length r_B=0,529177209 Å [16]. Apart from form factor and γ, its accuracy relies on the precision for m_e and m_P [10].

In (6), H radius r_0 is Bohr length r_B, corrected for recoil (7) or

$$r_0=[\hbar^2/(m_e e^2)](1+m_e/m_P)=0{,}5294654075 \text{ Å} \quad (16)$$

The ratio of classical natural H radius r_H in (15) and Bohr's r_0 in (16) is

$$x=r_H/r_0=1{,}391054876\ldots \quad (17)$$

(without recoil, r_H/r_B = 1,391812469….).

The natural virial Coulomb energy $-\frac{1}{2}e^2/r_H$ for any two charge-conjugated parts amounts to

$$\tfrac{1}{2}e^2/r_H=78844{,}900590508 \text{ cm}^{-1}=2363710654879{,}4 \text{ kHz} \quad (18)$$

When multiplied by (18), the conventional H asymptote (n=∞) is xe^2/r_H= 109677,583516024 cm^{-1}.

III. Scaling E_n by $\frac{1}{2}e^2/r_H$: probing Penrose's five-fold or φ-symmetry in atom H

Scaling E_n by natural H asymptote (18) gives numbers

$$N_n=E_n/(\tfrac{1}{2}e^2/r_H) \text{ or } nN_n=nE_n/(\tfrac{1}{2}e^2/r_H) \quad (19)$$

Due to (18), plots of nN_n versus 1/n and (1-1/n) in Fig. 1 give 4th order fits (with 5 decimals)

$$N_n=-0{,}00006/n^4+0{,}00007/n^3+1{,}39106/n^2 \quad (20)$$

$$N_n=-0{,}000056(1-1/n)^4+0{,}00015(1-1/n)^3+1{,}39093(1-1/n)^2-2{,}78210(1-1/n)+1{,}39107 \quad (21)$$

With (1-1/n), typical for molecular potentials [16], (20)-(21) reveal the effect of odd powers in 1/n, absent in Bohr $1/n^2$ theory and in a relativistic expansion in $E_n=\mu c^2(1/\sqrt{(1+\alpha^2/n^2)}-1)$ [8,14].

In (A16)-(A17), we prove that the H *force constant* k_n, away from critical configuration n_c, varies with 1,5/n. Fig. 1 includes N_n versus 1,5/n and (1-1,5/n) with 5-decimal 4th order fits

$$N_n=-0{,}00001(1{,}5/n)^4+0{,}00002(1{,}5/n)^3+\mathit{0{,}61825}(1{,}5/n)^2 \quad (22a)$$

$$N_n=-0{,}00001(1-1{,}5/n)^4+0{,}00002(1-1{,}(/n)^3+\mathit{0{,}61824}(1-1{,}5/n)^2-\mathit{1{,}23651}(1-1{,}5/n)+\mathit{0{,}61826} \quad (22b)$$

Coefficients of $(1,5/n)^2$ in (22a) and $(1-1,5/n)^2$ in (22b) are close to Euclid or Phidias number (10)

$$\varphi=\tfrac{1}{2}(\sqrt{5}-1)=1/\varphi-1=\Phi-1= 0{,}618034 \quad \ldots \quad (23)$$

Correction factor f_φ for φ-symmetry and f_r for recoil

$$f_\varphi=0{,}618247/0{,}618034-1=0{,}000344;\ f_r=m_e/m_P=1/1836{,}15267247=0{,}000545 \quad (24)$$

shows that f_φ is smaller than f_r by 40 %. Difference δ for φ-symmetry is 0,02 %, i.e.

$$\delta=0{,}618247-0{,}618034=0{,}000213 \quad (25)$$

In terms of ratio m_e/m_H=1/1837,15267247 in (7), difference (25)

$$(m_H/m_e)0{,}000213=0{,}390635\approx(9\varphi/4-1)=(9/4)(\tfrac{1}{2}\sqrt{5}-17/18) \quad (26)$$

reflects the importance of Euclid's golden ratio for H. Combining coefficient for 1,5/n (22a) and asymptotes 0,618247 in (22a-b) gives a 9-decimal result, close to ratio x in (18), since

$$x=(9/4).\ 0{,}618246619=(3/2)^2\varphi=1{,}391054894=r_H/r_0 \quad (27a)$$

Using (9), the Euclidean H variable x_E must obey

$x_E = a\varphi^{1/2}/n$ (27b)

Results (21)-(27) probe Penrose's five-fold or Euclid's φ-symmetry in H, due to alternative classical radius r_H (15). For internal φ-symmetry in H according to (13), (27) prescribes Euclidean variable

$X_E \sim x_E(1-x_E) \sim (a\varphi^{1/2}/n)(a\varphi^{1/2}/n-1)$ (28)

Given their smallness, of order recoil (13), only precise H terms [17-21] can provide with evidence for internal five-fold H symmetry (28).

IV. Putting φ to the test in H with accurate H intervals (prediction of H $1S_{1/2}$-$3S_{1/2}$)

The precision needed to validate (28) requires an upgrade of E_n [12]. Table 1 shows precise H terms available. Its 4 precisely known intervals A, B, D and E give 2 derived intervals C and F. Since only B and F are void of 1S, the immeasurable series limit or $-E_1$, B and F allow multiplicative scaling. Precision at this level requires many significant digits. A fit of E_n [12] to 4^{th} order in 1/n through the origin generates these digits and allows a test with terms in Table 1. Slope $1-1{,}79201817.10^{-8}$ and intercept 26940,95752/29979245,8=0,00008965361 cm^{-1} give the terms in kHz in Table 2. The conversion corresponds with a change of Erickson's 1977 R=109737,3177±0,00083 cm^{-1} [12].
Table 1 reveals that A, B and C are exactly reproduced. The small discrepancies for D, E and F are much lower than experimental uncertainties, 10 kHz for D and 21 for E in [20-21]. With the small error of 1,74 kHz for F removed, the error reappears for D and E (1,71 kHz). The small difference of 1,26 kHz for all terms caused by this correction justifies their omission in Table 2.
With ongoing experiments [11] in mind, we safely conclude that our predicted H 1S-3S interval (G in Table 1 and also in Table 2) is correct within 1,74 kHz, i.e. the largest error in Table 2.

Table 1 Observed [10] and intervals from this work in kHz (with errors δ). Prediction of H 1S-3S

Intervals[a,b]	Observed	This work	δ(kHz)	Ref[c].
A. 1S-2S	2466061413187,07	2466061413187,07	0,00	[17,18]
B. 2S-8S	770649350012,00	770649350012,00	0,00	[19]
C. [1S-8S]	3236710763199,07	3236710763199,07	0,00	
D. 2S-4S-¼(1S-2S)	4797338	4797334,20	-3,80	[20]
E. 2S-6S-¼(1S-3S)	4197604	4197601,94	-2,06	[21]
F. [6S-2S+¼(3S-2S)]	599734	599732,26	-1,74	
G. **1S-3S** predicted[d]	to be measured	**2922743278654,37**		[11]

[a] only B and derived F do not depend on 1S
[b] derived values between square brackets result from C=A+B and F=D-E
[c] the four intervals A,B,D,E are used for metrology in [10]
[d] by the same argument, all other intervals nS in Table 1 are predicted with the relative accuracy to reference term B [19]

Surprisingly, 4^{th} order is still sufficient to fit all data accurately, when 15 significant digits are used. $N_n = E'_n/(\frac{1}{2}e^2/r_H)$ plotted versus Euclidean variable x_E (27b) gives N_n, equal to

$-0{,}000028651871617x_E^4+0{,}000042968542402x_E^3+1{,}000344034289810x_E^2-0{,}000000000165642x_E$ (29)

For 19 terms 2S to 20S in Table 2, average errors of 0,11 kHz give a precision of $1{,}6.10^{-12}$ %. Small deviations ε_n nevertheless increase with increasing n (which we discuss elsewhere).
H terms in Table 2 allow a check of Euclidean variable X_E (28) for internal Euclidean φ-symmetry.

Table 2 H 1S-nS: original E_n [12] and converted E'_n in cm^{-1}, terms T_n in kHz and deviations ε_n with fitting to 4^{th} order (29)

n	$-E_n$ (cm^{-1})	$-E'_n$ (cm^{-1})	T_n (kHz)	ε_n(kHz)
1	109678,773704000	109678,77174307900	0	
2	27419,817835200	27419,81734379700	2466061413187,07	1,706
3	12186,550237200	12186,55001899660	2922743278654,37	0,139
4	6854,918845390	6854,91872213227	3082581563818,04	-0,078
5	4387,140880900	4387,14080222353	3156563684658,80	-0,097
6	3046,621950400	3046,62189584705	3196751430452,60	-0,083
7	2238,332451300	2238,33241135261	3220983339585,82	-0,065
8	1713,722059150	1713,72202861737	3236710763199,07	-0,050
9	1354,051221430	1354,05119731790	3247493423457,69	-0,038
10	1096,780974420	1096,78095487230	3255206191292,99	-0,029
11	906,430202530	906,43018635921	3260912763770,46	-0,022
12	761,652903990	761,65289037408	3265253077913,06	-0,016
13	648,982171840	648,98216020327	3268630861427,32	-0,012
14	559,581428918	559,58141885409	3271311028226,93	-0,008
15	487,457495457	487,45748665884	3273473249318,27	-0,005
16	428,429358101	428,42935033704	3275242868326,18	-0,003
17	379,508294780	379,50828787203	3276709484882,61	-0,001
18	338,511977355	338,51197116509	3277938523538,06	0,000
19	303,816802757	303,81679717463	3278978658687,20	0,001
20	274,194630876	274,19462581233	3279866709043,60	0,002
			average	0,124

V. Beyond Bohr H $1/n^2$ theory: probing internal φ-symmetry for fractal H

A 4^{th} order fit of accurate E'_n data in Table 2 exposes the contribution of Bohr's $1/n^2$ theory

$$-E'_n=-4{,}368336200714/n^4+5{,}555412530899/n^3+109677{,}583783388/n^2-0{,}000015348196n \quad (30)$$

Apart from small 1/n, subtracting term $1/n^2$ discloses accurate symmetry bound energy differences

$$\Delta E'_n=(4{,}368336200714/n^2-5{,}555412530899/n)/n^2\ cm^{-1} \quad (31)$$

Series limit E_1 in Table 2 gives $\Delta E'_n$, shifted by $1{,}18\ldots/n^2$. Coefficients in (31) reveal a parabola, obtained by adding $(½5{,}5554/\surd 4{,}3683)^2=1{,}32901^2=1{,}766268$. This hidden term in $1/n^2$ provides with a harmonic Rydberg R_{harm}, larger than R_∞ and R_1, in line with power fit (4) and is equal to [22]

$$R_{harm}=109677{,}583783+1{,}766268=109679{,}350051\ cm^{-1} \quad (32)$$

H symmetry equation (31) with R_{harm} now becomes a perfect Mexican hat curve, i.e. quartic [23]

$$\Delta_{harm}=(4{,}368336/n^2-5{,}555413/n+1{,}766268)/n^2\ cm^{-1}=1{,}766268(1-1{,}572642/n)^2/n^2 \quad (33)$$

which is critical at n=2.1,572642/n≈π≈4φ½ [23]. Fig. 2 gives quartics for R_{harm}, R_∞ and E_1 versus 4φ½/n-1. The more symmetrical Hund-type Mexican hat curve with R_{harm} (32) is an undeniable signature for left-right H behavior [23] but is usually, and unjustly, disregarded.

Using R_∞ to disclose internal H symmetries as in QED creates large energy differences (see Fig. 2). With (33) accurate to order kHz, Euclidean symmetry for fractal H is obvious. In fact, all numbers in (33) are sufficiently close to Euclidean variables (27)-(28), i.e.

$$9\varphi^{1/2}/4=1{,}768840600 \quad (34)$$

$$2\varphi^{1/2}=1{,}572302756 \quad (35)$$

transforming (33) in $9\varphi^{1/2}/4(1-2\varphi^{1/2}/n)^2/n^2$ and (31) in $9\varphi^{1/2}/4[1-(1-2\varphi^{1/2}/n)^2]/n^2$. For internal symmetry (35), the parts' ratio, the difference is only 0,000338763, just like 0,000344 in (24). This proves that internal H symmetry stems from chaotic/fractal behavior [4-5], Euclid's golden number [1-3] or Penrose's 5-fold symmetry [6], the most important, almost divine symmetry in nature [1-3].

VI. Discussion

(i) Spectral H data are accurately matched with a closed form quartic in 1/n. Unless for Lamb shifts, odd 1/n powers are absent in $1/n^2$ and QED theories. If observed data [13] had 5 decimals, QED data in [12] could have been avoided, since all main intervals in Table 1 are also available from [13]. Only the smaller intervals remain with an error (for F in Table 1, a persisting error of only 100 kHz suggests Kelly data have a wrong 4th decimal for 4S and/or 6S).

(ii) Euclidean H harmony rests on algebra, overlooked for recoil [16], see Section II.2. We agree with Cagnac et al. [14] that reduced mass as used in relativistic theories, see Section III, does not make sense. Using reduced mass instead of mass at n=∞ creates a huge error of about 60 cm^{-1}.

(iii) In the H_2 spectrum, natural asymptote $\frac{1}{2}e^2/r_H \approx 78844{,}9$ cm^{-1} shows as ionic energy $D_{ion}= e^2/r_H$ [16]: r_H is close to observed separation 0,74 Å in H_2 [24] and gives fundamental H_2 frequency of 4410 cm^{-1} [24]. With r_H and φ, molecular H_2 and atomic H spectra are intimately linked [16].

(iv) Incidentally, an angle of 30°, typical for Euclid's φ, also appears in the SM [25] as mixing angle for perpendicular interactions.

(v) Higher order terms in ξ=a/n or (1-ξ) brings H theory in line with Kratzer-type expansions like

$$E_n=a_0\xi^2\ (1+ a_1\xi + a_2\xi^2 + a_3\xi^3+\ldots) \quad (36)$$

formally similar to but different than the more familiar Dunham expansion [26-30].

(vi) Results for D and the H nP series are given elsewhere. With a Sommerfeld-Dirac fine structure formula [31], the internal variable for H nP is 1,5/n, rather than (35) for nS, which is responsible for the observed standard Lamb shift [22, 31].

Euclidean H-symmetry, brought about by natural radius r_H is in line with Rydberg's (1) and connects H terms with its most important property, mass m_H. H is not only prototypical for atomic and molecular physics [16]; it is prototypical for fractal behavior, in line with Mandelbrot [4]. We do not elaborate on discrete Euclidean geometries for composite H, conforming to Penrose 5-fold symmetry [6]. Bohr's model for composite H may well have to be refined on the basis of classical physics as suggested in Appendix A.

VII. Conclusion

Euclidean H symmetry only shows when H mass is directly linked to the H spectrum by virtue of its natural, classical radius r_H. Questions on conceptual, theoretical and practical (metrological) issues are outside the scope of this work. Definite conclusions depend on the observation of H 1S-3S [11].

References

[1] General references on phi are at http://en.wikipedia.org/wiki/Golden_ratio and in E.W. Weinstein, *Golden Ratio* at http://mathworld.wolfram.com . It is impossible to reference all articles on phi in peer reviewed journals by the authors, mentioned in [3-6] and by many others.
[2] M. Livio, The Golden Ratio: The Story of Phi, the World's most Astonishing Number, Broadway Books, New York, 20002
[3] A. Stahkov, *The Mathematics of Harmony*, World Scientific Publishing, Singapore, 2008
[4] B. B. Mandelbrot, *The Fractal Geometry of Nature*, Freeman New York, 1982
[5] M.C. Gutzwiller, Phys. Rev. Lett. **45**, 150 (1980)
[6] R. Penrose, *The Road to Reality*, Jonathan Cape, London, 2004
[7] J.S. Rigden, *Hydrogen: The Essential Element*, Harvard University Press, Cambridge, 2002
[8] M.I. Eides, H. Grotch and V.A. Shelyuto, Phys. Rept. **342**, 63 (2001)
[9] J.R. Rydberg, Kungl. Svenska Vet. Handl. **11**, 23 (1889)
[10] P.J. Mohr, B.B. Taylor and D.B. Newell, Rev. Mod. Phys. **80**, 633 (2008)
[11] O. Arnoult et al., Can. J. Phys. **83**, 273 (2005)
[12] G.W. Erickson, J. Phys. Chem. Ref. Data **6**, 831 (1977)
[13] R.L. Kelly, *Atomic and ionic spectrum lines below 2000 Angstroms. Hydrogen to Krypton*. New York, American Institute of Physics (AIP), American Chemical society and the National Bureau of Standards, 1987
[14] B. Cagnac et al., Rep. Prog. Phys. **57**, 853 (1994)
[15] B. de Beauvoir, Eur. Phys. J. D **12**, 61 (2000)
[16] G. Van Hooydonk, arxiv:0806.224
[17] M. Fischer et al., Phys. Rev. Lett. **92**, 230802 (2004)
[18] M. Fisher et al., in *Astrophysics, Clocks, and Fundamental Constants*, ed. S. Karshenboim and E. Peik, Lect. Notes Phys., **648**, 209 (2004)
[19] B. de Beauvoir et al., Phys. Rev. Lett. **78**, 440 (1997)
[20] M. Weitz et al., Phys. Rev. A **52**, 2664 (1995)
[21] S. Bourzeix et al., Phys. Rev. Lett. **76**, 384 (1996)
[22] G. Van Hooydonk, Phys. Rev. A **66**, 044103 (2002)
[23] G. Van Hooydonk, Acta Phys Hung NS **19**, 385 (2004)
[24] K.P. Huber and G. Herzberg, *Molecular Spectra, Molecular Structure: Constants of Diatomic Molecules*, vol. IV, Van Nostrand-Reinhold, New York, 1979
[25] P. Langacker, arxiv:0901.0241
[26] G. Van Hooydonk, Z. Naturforsch. A **37**, 710 (1982)
[27] G. Van Hooydonk, Spectrochim. Acta A **56**, 2273 (2000)
[28] G. Van Hooydonk, Eur. J. Inorg. Chem., Oct., 1617 (1999)
[29] G. Van Hooydonk, Eur. Phys. J. D **32**, 299 (2005)
[30] G. Van Hooydonk, Phys. Rev. Lett. **100**, 159301 (2008)
[31] G. Van Hooydonk, physics/0612141

Fig. 1 nN_n versus 1/n (Δ), 1-1/n (□) (solid lines), 1,5/n (+) and 1-1,5/n (x) (dashes).

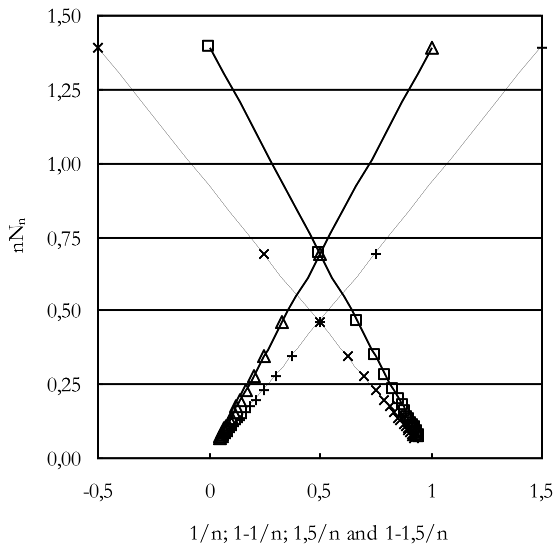

Fig. 2 Symmetry breaking curves in Euclidean H: E_n-differences (31)-(33) in cm^{-1} versus the appropriate Euclidean variable, see text): exact Mexican hat curve with R_{harm} (full-line □), E_1 (short dashes o) and NIST's R_∞ (broken dashes +)

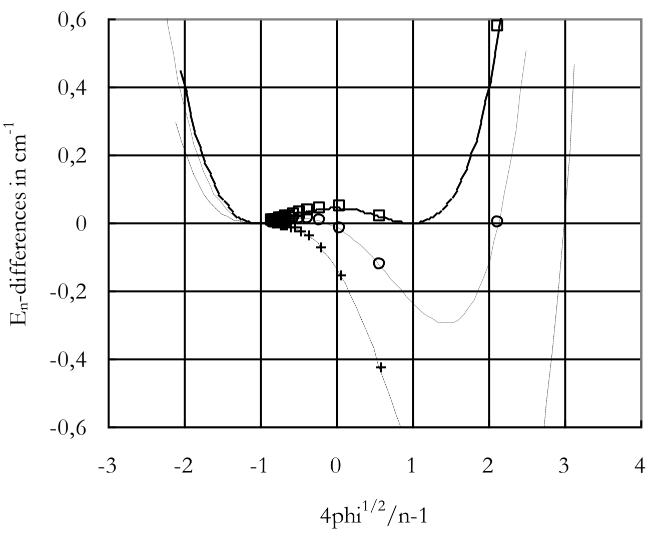

Appendix A Comparison of classical and Bohr H theories

This self-explanatory table contains all formulae for a stable charge-conjugated two particle Coulomb system, subject to periodic motion. Main results and differences are in bold.

Description	Classical H theory	Bohr H theory	#
Energy E=T+V	$E=\frac{1}{2}\mu v^2-e^2/r$	idem	A1
Hamiltonian	$E=\frac{1}{2}p^2/\mu-e^2/r$	idem	A2
Periodic motion	$E=\frac{1}{2}\mu\omega^2r^2-e^2/r$	idem	A3
Repulsive force d/dr	$\mu\omega^2r=\mu v^2/r=p^2/(\mu r)$	idem	A4
Attractive force d/dr	e^2/r^2	idem	A5
Equal forces (Newton)	$\mu v^2r=e^2$	idem	A6
Equal forces (Keppler, HO[a])	$\mu v^2=e^2/r$; $\mu\omega^2=e^2/r^3$; $\omega^2=e^2/\mu r^3$; $\omega=\sqrt{(k/\mu)}$	vibrator or HO not considered	A7
Force constant k_e at r_e	$k_e=e^2/r_e^3$	absent	A8
Constant periodicity dE/dω	$\mu\omega r^2=\mu vr=pr=C$	$\mu\omega r^2=\mu vr=pr=n\hbar$	A9
Moment	$p=C/r$	$p=n\hbar/r$	A10
Ratio A6/A9	$v=e^2/C$	$v=e^2/(n\hbar)$; $v/c=e^2/(n\hbar c)=\alpha/n$	A11
H radius	$r=C/(\mu v)=C^2/(\mu e^2)$	$r=n\hbar/(\mu v)= n^2\hbar^2/(\mu e^2)=n^2r_B$	A12
Feedback of A10 in E (A1)	$\frac{1}{2}p^2/\mu-e^2/r=\frac{1}{2}\mu v^2-\mu ve^2/C=\frac{1}{2}C^2/(\mu r^2)-\mu e^4/C^2=\frac{1}{2}e^2C^2/(\mu e^2r^2)-e^2/r$	$\frac{1}{2}\mu v^2-e^2/r=\frac{1}{2}\mu e^4/(n^2\hbar^2)-\mu e^4/(n^2\hbar^2)=-\frac{1}{2}\mu e^4/(n^2\hbar^2)=-R_H/n^2$	A13
Feedback to dE/dr=0 at r_0	$-C^2/(\mu r^3)+e^2/r^2$ or $C^2/\mu=e^2r_0$	absent	A14
Feedback to E (A13)	$E=\frac{1}{2}e^2r_0/r^2-e^2/r=\frac{1}{2}(e^2/r_0)[(r_0/r)^2-2r_0/r]$	absent	A15
Feedback to $d^2E/dr^2=k$	$k=3C^2/(\mu r^4)-2e^2/r^3=3e^2r_0/r^4-2e^2/r^3=2(e^2/r_0^3)(r_0/r)^3[1{,}5(r_0/r)-1]$	absent	A16
Classical r definition using n	$r=nr_0$	absent, replaced by A12 or $r=n^2r_B$	A17
Plugging (A17) in k (A16)	$k_n=k_1(1/n^3)(1{,}5/n-1)$; $k_1=e^2/r_0^3$	absent	A18
Plugging (A17) in E (A15)	$E=\frac{1}{2}(e^2/r_0)[1/n^2-2/n]$	absent	A19
Adding $E_0=\frac{1}{2}(e^2/r_0)$ to (A19)	$E'=E_0+\frac{1}{2}(e^2/r_0)[1/n^2-2/n]=E_0(1-1/n)^2$	absent	A20
Replacing 1/n by (1-1/n)	$E'=E_0[1-(1-1/n)]^2=E_0/n^2$	see result A13	A21
Energy difference, terms T_n	$T_n=E_0-E_0/n^2=E_0(1-1/n^2)$	$T_n=R_H-R_H/n^2=R_H(1-1/n^2)$	A22
Identical T formulae	n defined classically in (A17)	n in Bohr quantum hypothesis (A9)	A23

[a] HO is the classical Harmonic Oscillator

Force constant equations (A16)-(A18) for periodic motion and vibrations in HOs, are absent in Bohr theory. A switch to complementary variable (A21) is a switch from (i) energy $V=-e^2/r$ in (A1) to energy difference $\Delta V=-e^2/r+e^2/r_0$ and (ii) of moment $p=C/r$ in (A10) to moment difference $\Delta p=C(1/r-1/r_0)$. Kinetic and potential differences give $\Delta E=\frac{1}{2}(e^2/r_0)[\frac{1}{2}(1-1/n)^2-(1-1/n)]=\frac{1}{2}(e^2/r_0)/n^2$ (A21).
The usefulness of complementary variable 1-1/n in (A21), usually not considered for H theory, is illustrated by respective 4th order fits (2 digit version) of E'_n in Table 2

1/n: $E'_n=-4{,}37/n^4+5{,}55/n^3+109677{,}59/n^2-0{,}00/n+0{,}00$ cm^{-1}

(1-1/n): $E'_n=-4{,}37(1-1/n)^4+11{,}91(1-1/n)^3+109668{,}05(1-1/n)^2-219354{,}37(1-1/n)+109678{,}77$ cm^{-1}

Reducing H size classically in (A17) without a quantum theory gives the same results as Bohr's quantum hypothesis for angular momentum (A9).